

# The 94-GHz Cloud Profiling Radar For the CloudSat Mission

Eastwood Im, Stephen L. Durden, Chialin Wu, Thomas R. Livermore  
Jet Propulsion Laboratory  
California Institute of Technology  
4800 Oak Grove Drive, Pasadena, CA 91109  
818-354-0492  
eastwood.im@jpl.nasa.gov

*Abstract* — The CloudSat Mission is a new international satellite mission to acquire a global data set of vertical atmospheric cloud structure and its variability. Such data set is expected to provide crucial input to the studies of cloud physics, radiation budget, water distribution in the atmosphere, and to the numerical weather prediction models.

The key science instrument aboard the CloudSat satellite is the Cloud Profiling Radar (CPR). CPR is a 94-GHz nadir-looking radar that measures the power backscattered by clouds as a function of distance from the radar. This sensor is expected to provide cloud measurements at a 500-m vertical resolution and a 1.5-km horizontal resolution. CPR will operate in a short-pulse mode and will yield measurements at a minimum detectable sensitivity of -28 dBZ. In this paper, we will present the system design and the expected performance of this instrument, as well as the state-of-the art millimeter-wave technologies employed by this instrument.

## TABLE OF CONTENTS

1. INTRODUCTION
2. SYSTEM DESIGN
3. HARDWARE IMPLEMENTATION
4. CONCLUSIONS

## 1. INTRODUCTION

The CloudSat Mission [1] is a new satellite mission currently being developed by the National Aeronautics and Space Administration (NASA), the Jet Propulsion Laboratory (JPL), and the Canadian Space Agency (CSA) to acquire a global data set of vertical cloud structure and its variability. . Such data set is expected to provide crucial input to the studies of cloud physics, radiation budget, water distribution in the atmosphere, and to the numerical weather prediction models. The CloudSat Mission is planned to launch together with another cloud measurement mission called PICASSO-CENA [2] in early summer of 2003. During normal operations, the two missions will fly

in formation to provide detailed, multi-parameter measurements of the 3-dimensional cloud field over the entire globe.

One key science instrument aboard the CloudSat satellite is the Cloud Profiling Radar (CPR). CPR is a 94-GHz nadir-looking radar that measures the power backscattered by clouds as a function of distance from the radar. These data will provide an along-track vertical profile of cloud structure. Figure 1 shows the operational geometry of CPR. In this paper, we will present the system design and the expected performance of this instrument, as well as the state-of-the art millimeter-wave technologies employed by this instrument.

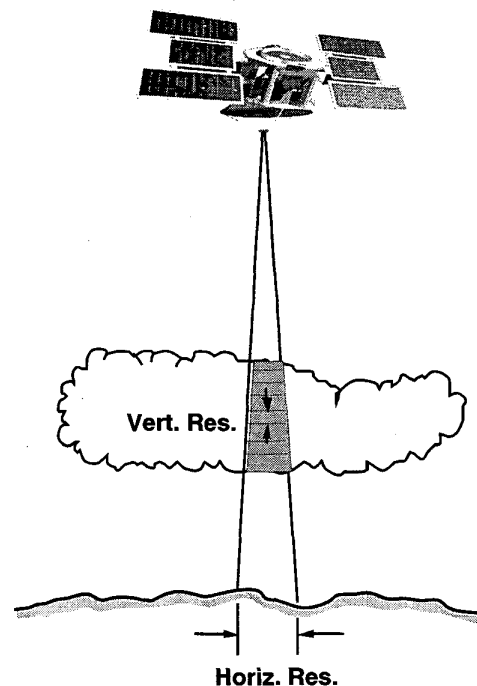


Figure 1. Cloud Profiling Radar (CPR) operational geometry.

## 2. SYSTEM DESIGN

The design of CPR is driven by the CloudSat science objectives. The primary science objective is a minimum detectable cloud reflectivity ( $Z$ ) of -26 dBZ<sup>1</sup> at the end of the mission. This performance is needed since clouds are weak scatterers. By comparison the reflectivity for rain is typically 20-50 dBZ; the Tropical Rainfall Measuring Mission (TRMM) Precipitation Radar (PR) [3] has a sensitivity of around +20 dBZ.

Maximizing the cloud detection sensitivity requires careful tradeoff among several competing and often conflicting parameters, including the cloud backscattering sensitivity, atmospheric absorption, resolution, and radar technology. The detection sensitivity is primarily determined by the radar received power and the noise level. The radar received power can be written as [4]

$$P_a(r) = \frac{P_t \lambda^2 G^2 \theta^2 \Delta \eta L}{512 \pi^2 \ln 2 r_a^2} \quad (1)$$

where  $P_t$  is the transmitter power,  $\lambda$  is the wavelength,  $G$  is the antenna gain,  $\theta$  is the antenna half-power beamwidth,  $\Delta$  is range resolution,  $r_a$  is the range to the atmospheric target,  $\eta$  is the cloud reflectivity<sup>1</sup>, and  $L$  is the signal loss.  $P_a(r)$  is the received power from the atmosphere versus range. The product  $G^2 \lambda^2 \theta^2$  is proportional to the antenna effective area. Thus, the received power is increased by increasing antenna area, range resolution, transmit power, and reflectivity. The antenna size is limited by the physical launch constraints such as volume and mass. Transmitted power is limited by the technology of the transmitter itself and by the power supply capability of the spacecraft.

The amount of power received is strongly influenced by the the interactions between the atmosphere and the intervening electromagnetic waves. Such interactions can be characterized by two key parameters: the cloud reflectivity and the atmospheric absorption. In general, the cloud reflectivity increases by increasing the radar frequency. In the Rayleigh regime at which the cloud particles are small relative to the radar wavelength, the cloud reflectivity increases as  $\lambda^4$ . In this case, the cloud droplets are relatively transparent at centimeter wavelengths, and millimeter wavelengths are required for cloud observations.

On the other hand, signal absorption due to atmospheric gases may be prohibitively large at smaller wavelengths (i.e., higher frequencies). The atmospheric absorption spectrum [5], [6] as shown in Figure 2 indicates that the spectral windows suitable for cloud observations are around 35, 94, 140 and 220 GHz. From these considerations, the use of 94 GHz provides an increase of 33 dB as compared with the use of the TRMM PR frequency of 14 GHz. Even at 35 GHz the required transmit power and/or antenna size

<sup>1</sup> dBZ is dB relative to 1 mm<sup>6</sup>/m<sup>3</sup>. These are the units of  $Z$ , known as reflectivity or more properly reflectivity factor.  $Z$  is proportional to the reflectivity  $\eta$ , which is the radar cross section per unit volume, measured in units of m<sup>1</sup>

exceeds limitations of technology and cost. Frequencies above 100 GHz provide an additional increase in sensitivity; however, technology is not mature enough for a spaceborne radar. The use of 94 GHz for the CPR thus allows the sensitivity requirement to be met using available technology.

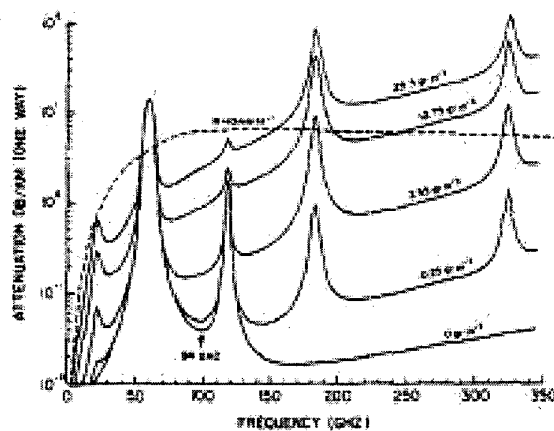


Figure 2. Atmospheric gases absorption spectrum for various humidity conditions and due to 10 mm/hr rain [5], [6].

Sensitivity is also related to the pulse length ( $\tau$ ); longer pulse lengths provide better sensitivity but poorer vertical resolution. CPR will operate using 3.3- $\mu$ s monochromatic pulses to provide the required sensitivity while also meeting the range resolution requirement of 500 m. The required vertical resolution can be maintained when using longer pulses by employing pulse compression techniques [7], [8]. In this case a frequency-modulated chirp is transmitted and the received signal is compressed by correlation with a replica of the transmitted signal. While pulse compression can be used to enhance the vertical resolution, it has the disadvantage of creating range sidelobes. For CPR, the required sidelobe suppression to make the chirp data useful down to the surface is at least 75 dB, probably greater for a smooth ocean surface. This is considered beyond the current state of the art. Hence for CPR only a conventional 3.3- $\mu$ s monochromatic pulse is used. To maximize power, the short pulse must have rapid rise and fall times and minimal droop.

The other approaches for improving sensitivity involve reducing noise from various sources. Thermal noise is generated by the finite antenna temperature and receiver temperature. The receiver noise is minimized by using a low noise amplifier and by reducing the losses between the antenna and the low noise amplifier. The total noise power also depends on receiver bandwidth, so matching the receiver bandwidth to the transmit bandwidth provides an optimal SNR while maintaining the required resolution. The optimal 6 dB bandwidth is approximately 1.1-1.2 times the reciprocal of the pulse length. For 3.3- $\mu$ s rectangular pulse, the matched filter should have a 6 dB

bandwidth of 330-360 kHz. The maximum expected Doppler shift due to a pointing off nadir of  $0.1^\circ$  is 8 kHz. In this case the receiver 6 dB bandwidth should be 376 kHz. An additional source of shifting is a change in the radar STALO during the roundtrip time. To keep this below 1 kHz, the STALO frequency must not change by more than  $1.0 \times 10^{-8}$  in 5 ms (the STALO's Allen deviation requirement). Including margin for Doppler shifting we find that the 6 dB filter should be 350-380 kHz. For a Gaussian shape this corresponds to a 3 dB width of around 270 kHz. Unfortunately, because of the detection scheme this filter must be implemented at a center frequency of 50-100 MHz. Such a narrow band filter is difficult, so the current specification is 320 kHz. Besides the receiver filter bandwidth, the shape must also be carefully considered. A filter with too sharp a cutoff would cause time domain ringing, causing the signal at one range bin to interfere with the signal at another. Ripple in the filter response also increases the mismatch and is undesirable. Simulations have shown that no more than 1 dB can be tolerated.

The thermal noise contribution is further reduced by averaging many samples of the measured power and subtracting the estimated noise level. The sensitivity improvement due to noise subtraction is proportional to the square root of the number of independent samples. The number of independent samples can be increased by increasing the pulse repetition frequency (PRF). However, the maximum PRF is set by range ambiguity considerations. For CPR, the nominal range window size is set at 30 km, allowing capture of the surface return and cloud return up to an altitude of 25 km. System noise level is estimated using the clear air radar return from 25 to 30 km altitude. A data window of 30 km allows a maximum PRF of 5000 Hz. However, because the altitude varies over the orbit, such a high PRF would require continuous updating. Instead, a PRF of around 4300 Hz is used. The exact PRF varies with altitude to satisfy the constraint that the received data window not overlap the transmit event. In particular, if the roundtrip time is  $T_o$  and the length of the data window is  $T$ , then the data window position (DWP) is  $T_o - (n-1)PRI - T$ , where  $PRI$  is the inverse of the PRF and  $n$  is the number of echoes in flight. The constraint on transmit versus receive is satisfied if  $DWP > \tau$  and  $DWP < PRI - T$ , including some margin for switching from transmit to receive.

In the baseline design, the radar measurements along the nadir track are averaged in 0.32-sec time intervals. This corresponds to an effective along-track horizontal resolution of 3.5 km (i.e.,  $0.3 \text{ s} \times 7 \text{ km/s} + 1.4 \text{ km}$ ) on the CPR measurements after averaging. In order to provide enhanced capability to discriminate cloud features, the CPR measurements are sampled at 250-m in range, and 0.16 s along the nadir track. The 0.32 s averaging at 4300 Hz provides nearly 1400 samples for averaging. These samples are independent since the satellite moves 1.6 m between each pulse, which is substantially more than one-half the antenna diameter (1 m). The noise subtraction approach should allow signals that are 15 dB below the thermal noise to be detected.

In addition to thermal noise, the backscattered signal may be contaminated by surface clutter through antenna sidelobes or pulse compression sidelobes. For a nadir-pointed antenna, the primary clutter source is the surface return from previously transmitted pulses that are received through the antenna sidelobes. If the range to the cloud is  $r_a$ , then all points on the surface with range  $r_s$  is equal to  $r_a + nc/2PRF$  will contribute. As discussed in [9], the surface clutter through sidelobes for a given  $n$  is due to an annulus on the earth's surface. The power received from the annulus  $P_s$  can be written as a surface integral over the azimuth angle  $\phi$  and the angle  $\gamma$  between the earth radius to the nadir point and the earth radius to the annulus (shown in Figure 3). This integral can be simplified [9], giving the following expression for  $P_s$ ,

$$P_s(r) = \frac{P_t \lambda^2 G^2 R_e (r_2^2 - r_1^2) \sigma^\circ}{128 \pi^3 (R_e + h) r_s^4} \int g^2(\theta, \phi) d\phi \quad (2)$$

where  $R_e$  is the earth's radius,  $h$  is the spacecraft altitude,  $r_1$  and  $r_2$  are the ranges to the inner and outer edges of the annulus,  $\sigma^\circ$  is the surface cross section, and  $g(\ )$  is the antenna pattern. The signal-to-clutter ratio (SCR) can be computed as the ratio of the power from the atmosphere (Eq. (1)) to the sum of power from all surface annuli (Eq. (2)). The number of the maximum annulus corresponds to the edge of a spherical earth model, while the minimum value corresponds to nadir return, and for nadir-looking radars, the minimum value of is 0.

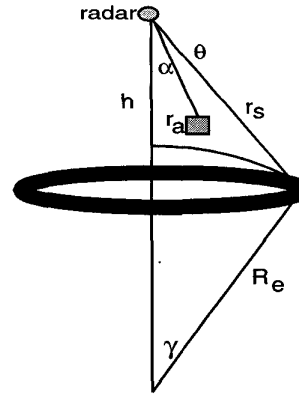


Figure 3. Surface clutter geometry for spaceborne atmospheric radars.

The SCR depends on both the surface clutter and the atmospheric return. We can solve for the minimum detectable  $Z$  due to clutter, defined as that  $Z$  having an SCR of unity. Figure 4 shows the minimum detectable reflectivity factor  $Z$  versus altitude for antenna sidelobe levels of -38 dB and -50 dB. The calculation is for land surface clutters. For the CPR geometry, the clutters coming from angles less than  $7^\circ$  have minimal contributions to the overall clutter noise. Our calculations show that an antenna with a -50-dB sidelobe level at angles  $>7^\circ$  is adequate to suppress the surface clutters, while a -38 dB level is not. This clutter model allows the establishment of

the antenna sidelobe requirements. For a given an antenna sidelobe level, the surface clutter can be further suppressed using a frequency diversity scheme. In this frequency diversity approach, the transmitter transmits a sequence of pulses with carrier frequencies that are appropriately separated. The receiver tracks these frequencies, so that the desired echo from clouds is within the receiver bandwidth, while surface return from previous pulses leaking through antenna sidelobes is outside the receiver bandwidth. Calculations have shown that this approach provides sufficient clutter suppression even for a land surface and an antenna with constant -38 dB sidelobes (Figure 4). For CPR, the predicted antenna sidelobes beyond 7° from boresight are below -50 dB. Hence, frequency diversity is not needed. However, the frequency diversity approach has been kept as a backup in case the actual antenna performance falls short of expectation.

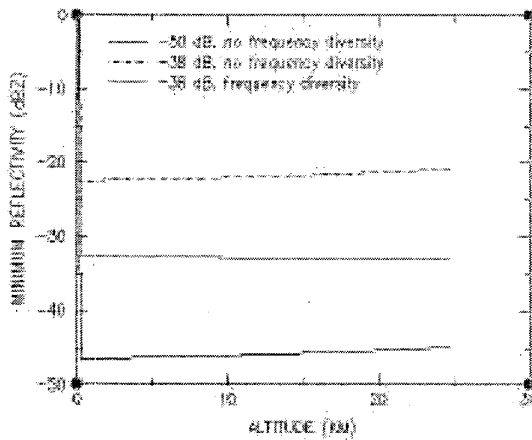


Figure 4. Minimum reflectivity factor Z due to clutter.

The planned operational scenario calls for continuous radar science data acquisition. Table 1 shows the expected functional and performance parameters of CPR during normal operations.

Table 1. CPR system parameters.

Frequency	94.05 GHz
Altitude	720 km
Range resolution	507 m
Cross-track resolution	1.4 km
Along-track resolution	3.5 km
Pulse width	3.33 $\mu$ s
Peak power (end of life)	1.6 kW
PRF	4000 Hz
Antenna diameter	1.85 m
Antenna gain (dBi)	62 dBi
Antenna sidelobes	-50 dB @ $\theta > 7^\circ$
Integration Time	0.48 sec
Data window	0 – 25 km
Minimum detectable reflectivity	-28 dBZ

Science requirements call for an absolute calibration of CPR to 2 dB. This is accomplished by making frequent estimates of the transmit power by a power meter, and by frequent receiver gain monitoring through periodically coupling of the output of a noise diode into the receiver. These measurements, along with pre-launch measurements of the antenna pattern and transmit and receive path losses, are used by the ground data processing system to calibrate the data. Calibration accuracies are also monitored by examining ocean surface backscatter.

Figure 5 shows the internal calibration scheme for CPR. The calibrated radar cross section per unit volume (reflectivity) can be found from

$$\eta = \frac{P_r (4\pi)^3 r_a^2}{P_t G^2 \lambda^2 \Delta \Omega} \quad (3)$$

where  $\Omega$  is the integral of the normalized two-way antenna pattern. The antenna gain and  $\Omega$  are estimated from antenna range measurements.  $\Delta$  is determined from laboratory measurements of the received pulse shape. The transmit power  $P_t$  is determined from the power detector, which samples a small amount of the transmit power from the antenna. Received power  $P_r$  is determined from  $P_{r0}$  and from receiver gain measured by periodic coupling of known noise diode into receiver.

Our current estimate of the calibration errors, including both pre-launch measurement error, launch effects, and the post-launch calibration stability, is  $\sim 1.7$  dB. This accuracy can be further improved through external calibration measurements during both pre- and post-launch phases.

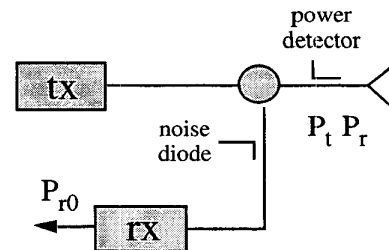


Figure 5. CPR internal calibration approach.

### 3. HARDWARE IMPLEMENTATION

CPR is implemented by the following subsystems: Radio Frequency Electronics Subsystem (RFES), High-Power Amplifier (HPA), Antenna, and Digital Subsystem (DSS). The simplified version of the CPR instrument block diagram is shown in Figure 6. The RFES consists of an upconverter which accepts a 10 MHz oscillator signal from the DSS and upconverts it to a pulse-modulated 94 GHz signal. The signal is amplified to approximately 200 mW by a MMIC power amplifier. A switch within the

upconverter is used to provide the modulation for generating pulses. The receiver accepts the received signal from the antenna and downconverts it to an intermediate frequency (IF). A MMIC low-noise amplifier (LNA) provides the first stage of amplification. The gain of the LNA is large enough that additional stages have only a small contribution to the system noise temperature. The IF signal following downconversion is detected using a logarithmic amplifier; this approach has been used on the TRMM PR to provide high dynamic range [3].

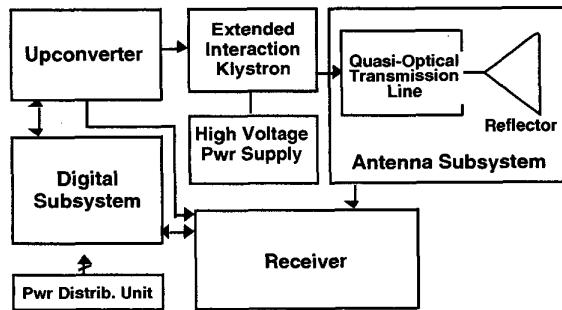


Figure 6. Simplified CPR block diagram.

The HPA, which amplifies the transmitted pulse to a nominal power level of 1.7 kW, consists of an extended interaction klystron (EIK) and a high-voltage power supply (HVPS). Both a primary and a backup HPA are used to enhance system reliability. The EIK tube is a space-qualified version of a commercial tube, manufactured by Communications and Power Industries, Canada, Inc. This family of EIKs has been used extensively in existing ground-based and airborne 94 GHz cloud radars [10]. The EIK differs from standard klystrons by using resonated bi-periodic ladder lines as a replacement for conventional klystron cavities. The EIK provides a large peak power in a very compact and lightweight package. The high-voltage power supply (HVPS) provides the voltages needed to operate the EIK (heater, cathode, collector and modulator) and provides telemetry data necessary to system needs. The design uses a boost supply to minimize input current transients during the pulsing period and control EMC problems.

In order to ensure adequate mitigation of the 94-GHz HPA technology risks in the CPR program, in 1999 the first engineering model for the EIK was built and tested for structural integrity. In 2000, the second EIK engineering model was built and is currently undergoing environmental testing. This second EIK unit is shown in Figure 7. In addition, the breadboard model for the HVPS was also built in 2000 and its performance was verified. This HVPS breadboard model is shown in Figure 8.

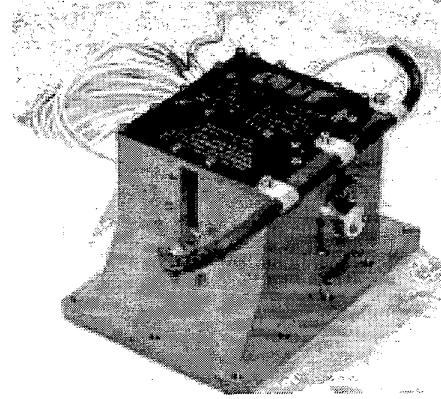


Figure 7. The second engineering model of the CPR's 94-GHz Extended Interaction Klystron tube.

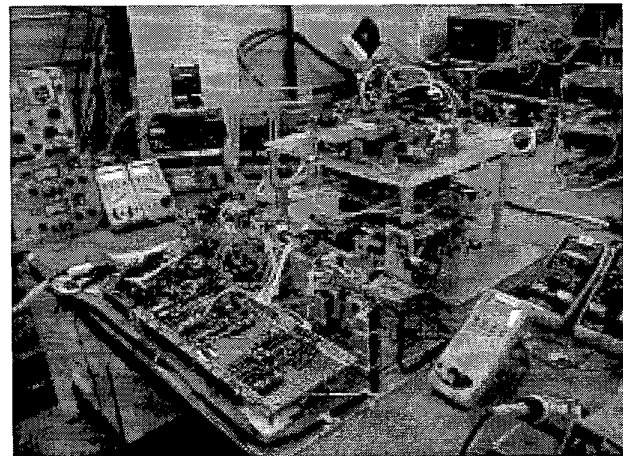


Figure 8. The breadboard model of the CPR's 94-GHz High-voltage Power Supply.

The CPR Antenna Subsystem consists of the collimating antenna reflector and the quasi-optical transmission line (QOTL) [11]. The collimating antenna is a fixed 1.85-m diameter reflector, made from space-qualified composite graphite material to reduce mass. The antenna provides more than 63 dBi gain, has beamwidth  $< 0.12^\circ$ , and has sidelobes less than -50 dB for angles greater than or equal to  $7^\circ$  from boresight. This low sidelobe level is achieved using an offset feed design. In stead of using conventional waveguide, the antenna is fed by the QOTL for low loss. This QOTL approach is based on free-space transmission of Gaussian RF beams, with beam direction and focusing achieved by shaped metallic mirrors. The CPR Antenna Subsystem is graphically illustrated in Figure 9.

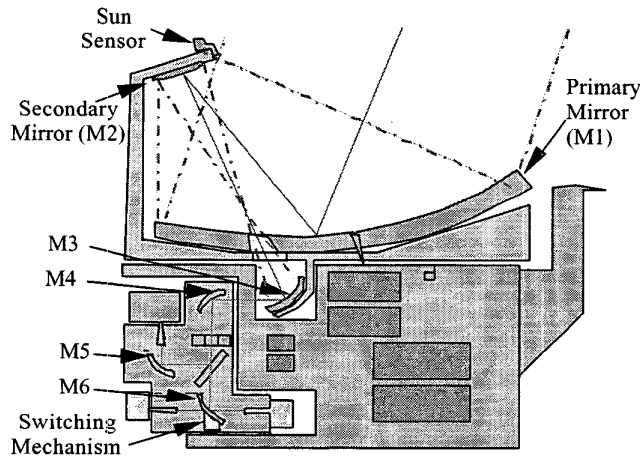


Figure 9. Graphical illustration of the CPR Antenna Subsystem.

The DSS provides the following functions: (1) to receive commands from the spacecraft and transmit them in the correct format to the rest of the radar; (2) to digitize the telemetry from the rest of the radar and incorporate the digitized words in the science and telemetry data streams; (3) to digitize the radar echo, do simple data processing and transmit the data to the as part of the science data stream to be downlinked to earth; (4) to generate the radar timing signals including the STALO; (5) to generate the radar signal that will be upconverted from L-Band to 94 GHz in the RFES and transmitted by the HPA. The first four functions are done in the Control and Timing Unit (CTU) portion of the DSS. The Digital Data Handler (DDH) accepts the analog signal from the RFES logarithm detector.

It digitizes the signal and performs the required averaging at each of 125 range bins. The averaged power is converted to a floating point format prior to being sent to the solid state recorder. The use of floating point reduces the required number of bits and data rate. Owing to its simplicity, much of the DSS is implemented using FPGAs. No flight computer or flight software is used by DSS in order to reduce development time and cost.

Power for CPR is provided by a Power Distribution Unit (PDU). The PDU accepts the nominal 28V DC prime power from the spacecraft, and converts the 28V input to appropriate secondary DC voltages to operate those lower voltage electronics subsystems. The PDU is based on commercial off-the-shelf power supplies. The PDU supplies power to the RFES, DSS, and the antenna subsystem (HPA selection switch). The HPA's accept the 28 V power from the spacecraft directly. The spacecraft also directly supplies 28 V power to replacement heaters. These will be operated whenever the radar is off, in order to maintain the electronics at temperatures within the survival range.

#### 4. CONCLUSIONS

The Cloud Profiling Radar (CPR) on the CloudSat mission will provide the first global view of the vertical structure of clouds. It is a nadir-looking radar operating at 94 GHz. While the radar is fairly straightforward from a functional point of view, the required technology at millimeter wave frequencies presents some challenges. A design has been developed which meets the requirements and can be implemented using available technology. The design, as known during the formulation phase, has been presented. This design is undergoing some refinement. CPR will be implemented during the next two years, in preparation for a launch in 2003.

#### ACKNOWLEDGMENTS

The authors would like to thank the members of the CloudSat Cloud Profiling Radar Engineering Team for providing the critical technical data and for review of this paper. The research described in this paper was performed at the Jet Propulsion Laboratory, California Institute of Technology, under contract with the National Aeronautics and Space Administration.

#### REFERENCES

- [1] G. L. Stephens, D. G. Vane, and S. J. Walters, "The CloudSat Mission: a new dimension to space-based observations of cloud in the coming millenium," GCSS-WGNE Workshop on Cloud Processes and Feedbacks in Large Scale Models, 1998.
- [2] D. M. Winker, and B. A. Wielicki, "The PICASSO-CENA Mission," Sensors, Systems, and Next Generation Satellites, H. Fujisada, Ed., *Proc. SPIE*, 3870, 2000.
- [3] T. Kozu, T. Kawanishi, H. Kuroiwa, M. Kojima, K. Oikawa, H. Kumagai, K. Okamoto, M. Okumura, H. Nakatsuka, and K. Nishikawa, "Development of precipitation radar onboard the Tropical Rainfall Measuring Mission (TRMM) satellite," *IEEE Trans. Geosci. Remote Sensing*, accepted for publication.
- [4] J. R. Probert-Jones, "The radar equation for meteorology," *Quart. J. Royal Meteor. Soc.*, 88, 485-495, 1962.
- [5] H. J. Liebe, "An updated model for millimeter-wave propagation in moist air," *Radio Sci.*, 20, 1069-1089, 1985.
- [6] R. Lhermitte, "A 94-GHz doppler radar for cloud observations," *J. Atmos. Oceanic Technol.*, 4, 36-48, 1987.

[7] E. Im, S. Durden, F. Li, A. Tanner, and W. Wilson, "Pulse compression technique for spaceborne precipitation radars," *Proc. 11th Intl. Conf. on Clouds and Precip., Montreal, Canada, 1079-1082, 1992.*

[8] A. Tanner, S. L. Durden, R. Denning, E. Im, F. K. Li, W. Ricketts, W. Wilson, "Pulse compression with very low sidelobes in an airborne rain mapping radar," *IEEE Trans. Geosci. Remote Sensing, 32, 211-213, 1994.*

[9] S. L. Durden, E. Im, F. K. Li, and R. Girard, "Surface clutter due to antenna sidelobes for spaceborne atmospheric radar," submitted to *IEEE Trans. Geosci. Remote Sensing.*

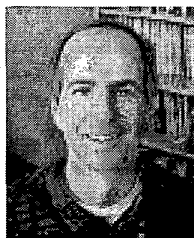
[10] G. A. Sadowy, R. E. McIntosh, S. J. Dinardo, S. L. Durden, W. N. Edelstein, F. K. Li, A. B. Tanner, W. J. Wilson, T. L. Schneider, G. L. Stephens, "The NASA DC-8 Airborne Cloud Radar: Design and Preliminary results," *Proc. IGARSS'97, F02.6., 1997.*

[11] S. Spitz, A. Prata, J. Harrell, R. Perez, and W. Veruttipong, "A 94 GHz Spaceborne Cloud Profiling Radar Antenna System," *2001 IEEE Aerospace Conference Proceedings, March 10-17, 2001.*

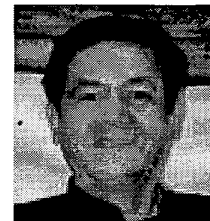
**Dr. Eastwood Im** is the Radar Instrument Manager of the NASA ESSP CloudSat Mission. He is also the Supervisor of the Atmospheric Radar Science and Engineering Group at JPL. He has extensive experience in spaceborne meteorological radar science and remote sensing, and advanced radar system studies. Dr. Im is the Principal Investigator of the TRMM radar calibration study and a member of the TRMM Science Team, and the Principal Investigator of the NASA IIP Second-Generation Precipitation Radar (PR-2) task. He has been a member of Science Steering Group for the EOS-9 Global Precipitation Mission since the start of the planning phase. Dr. Im is the Associate Editor of the AMS Journal of Atmospheric and Oceanic Technology. He has over 80 refereed journal and conference publications.



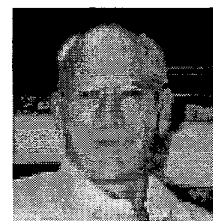
**Dr. Stephen L. Durden** is a Principal Engineer at JPL and has contributed to the development of Airborne Rain Mapping Radar and Airborne Cloud Radar, and to the design of spaceborne synthetic aperture radar (LightSAR). He is a member of the TRMM Science Team Postlaunch Validation Team, and the System Engineer for both the 94-GHz Cloud Profiling Radar for the ESSP CloudSat Mission, and the IIP Second-Generation Precipitation Radar prototype. He has also been actively engaged in microwave remote sensing research, including modeling of microwave scattering and data analysis. He is author or co-author of over 35 journal publications.



**Dr. Chialin Wu** is a Principal Engineer at JPL, and is the Instrument Engineer of the Cloud Profiling Radar on the NASA CloudSat Mission. Previously, he was the Experiment Engineer of the SeaWinds radar scatterometers on the QuikScat and the ADEOS II (of Japan) Missions. Prior to the scatterometer instrument development, he served as deputy manager and system engineering chief of the Radar Office on the Magellan Mission to Venus, and as a member of the SAR Team on the Seasat Mission. He has published many papers and five US Patents in the field of radar systems and signal processing. The two patents on digital SAR processor with clutterlock, and on SAR interferometer for contour mapping, won major NASA awards.



**Tom R. Livermore** has thirty years of experience in development of systems for aerospace, commercial and military markets. Currently, Mr. Livermore is the Project Manager for the CloudSat Mission, an Earth orbiting mission designed to measure the vertical structure of clouds and quantify their ice and water content. The CloudSat Mission will launch in 2003. Most recently, he was the Project Manager for the Multi-angle Imaging SpectroRadiometer (MISR), a key instrument on the Terra spacecraft, the first EOS mission launched in December, 1999. He was the Project Manager for the Integrated Multispectral Atmospheric Sounder (IMAS) proposal efforts. IMAS is an Earth-orbiting design integrating millimeter-wave and infrared sensors to provide 1 degree, 1 km resolution for atmospheric sounding. Prior to IMAS, Mr. Livermore led the Space Interferometry Mission Pre-Project effort, resulting in a Phase A start for the SIM Mission. He also managed the development and delivery of the Cassini Imaging Science Subsystem, comprising a wide angle and a narrow angle camera that are integrated into the Cassini spacecraft, currently en-route to Saturn for a 4 year tour. Mr. Livermore managed the development of the Drive and Control system for the W. M. Keck Observatory 10 Meter Telescope, from 1985-1990. His other scientific work included two years managing the electronics section at the world's largest radio telescope at Arecibo, Puerto Rico. His background also includes development of mmW radar and passive sensors, control systems and commercial electronics development.



This page intentionally left blank.